High resolution photoelectron imaging of Au2

Iker León, Zheng Yang, and Lai-Sheng Wang

Citation: The Journal of Chemical Physics **138**, 184304 (2013); doi: 10.1063/1.4803477
View online: http://dx.doi.org/10.1063/1.4803477
View Table of Contents: http://scitation.aip.org/content/aip/journal/jcp/138/18?ver=pdfcov
Published by the AIP Publishing

High resolution photoelectron imaging of Au_2^-

Iker León, Zheng Yang, and Lai-Sheng Wang[a)]
Department of Chemistry, Brown University, Providence, Rhode Island 02912, USA

(Received 20 March 2013; accepted 17 April 2013; published online 8 May 2013)

We report high resolution photoelectron spectra of Au_2^- using a newly built photoelectron imaging apparatus. Vibrationally resolved photoelectron images are obtained for the ground state detachment transition of Au_2^- at various photon energies (442.80–670.18 nm) at a resolution of 3 cm^{-1} for low energy electrons. Franck-Condon simulations yield the vibrational temperature of Au_2^- and the high resolution data yield accurate spectroscopic constants for the ground states of Au_2 and Au_2^-. The electron affinity of Au_2 is measured to be 1.9393 ± 0.0006 eV. A more precise value for the Au_2^- dissociation energy is also obtained as 1.937 ± 0.005 eV. © *2013 AIP Publishing LLC*. [http://dx.doi.org/10.1063/1.4803477]

Anion photoelectron spectroscopy (PES) has proven to be a powerful technique for the study of size-selected atomic clusters. It probes directly the electronic and, in some cases, vibrational structures of the corresponding neutral species. However, the resolution of PES is limited to a few meV in the best cases, which is not sufficient to resolve low frequency vibrations. Zero electron-kinetic-energy (ZEKE) spectroscopy can reach much higher resolution of a few cm^{-1} or even sub-wavenumbers.[1–4] But its application to anions[5–8] has been limited because of the threshold law,[9] which favors detachment of *p*-like electrons with *s* outgoing waves. Photoelectron imaging allows very low energy electrons to be detected, providing a much higher resolution method for PES. The imaging technique was originally developed to record spatial distributions of photodissociation products,[10] but was soon applied to photoelectrons from multiphoton ionization of Xe and size-selected cluster anions.[11,12] With the development of the velocity map imaging (VMI) technique by Eppink and Parker,[13] photoelectron imaging has evolved into a powerful alternative PES method over the past decade.[14–20] The advantage of photoelectron imaging lies at its high detection efficiency while yielding photoelectron angular information at the same time. The sensitivity of the imaging method to slow-electrons has allowed high-resolution photoelectron spectra to be obtained for near zero-eV electrons.[21,22] The latter is known as SEVI by the Neumark group for slow electron velocity-map imaging.[23] More recently, rotational resolution has been reported for slow electron imaging of small neutral molecules using multiphoton ionization.[24]

We designed previously a photoelectron imaging system to study the angular distributions of multiply charged anions from an electrospray ionization source.[25,26] Recently, we have developed a high resolution photoelectron imaging system for the study of size-selected cluster anions produced from a laser vaporization supersonic cluster source. In the current work, we present our first result on Au_2^- as a test case reporting a more accurate value of the electron affinity (EA) and more accurate spectroscopic constants for the anion. Au_2^- was selected because of its well-known spectroscopy.[7,27–33] In particular, a vibrationally resolved PES spectrum of Au_2^- was first reported by Lineberger and co-workers using a hemispherical electron analyzer at a resolution of ~6 meV and a vibrational temperature of 350 ± 25 K.[28] Gantefor and co-workers reported a ZEKE spectrum of Au_2^- in the photon energy range of 1.85 to 2.025 eV at a spectral resolution of 1.5 meV and a vibrational temperature of 165 ± 30 K.[7] In the current work, we report photoelectron images of Au_2^- in the photon energy range of 1.8470 eV (671.28 nm) to 2.8000 eV (442.80 nm) at a vibrational temperature of 175 ± 25 K and a kinetic energy resolution of 2.8 cm^{-1} for slow electrons.

Details of the new apparatus will be published separately. Briefly, the laser vaporization supersonic cluster source and the time-of-flight mass spectrometer are similar to our magnetic-bottle apparatus, which were described in detail before.[34] A gold disk was used as the laser vaporization target with a helium carrier gas seeded with 5% argon, which produces relatively cold gold cluster anions.[35] Clusters formed inside the nozzle were entrained by the carrier gas and underwent a supersonic expansion. After a skimmer, anions from the collimated cluster beam were extracted perpendicularly into a time-of-flight mass spectrometer. The Au_2^- dimer of current interest was mass-selected and focused into the collinear VMI system. The VMI lens is based on the design by Suits and co-workers for ion imaging,[36] which is modified and optimized for photoelectron imaging. Photoelectrons are accelerated toward a position-sensitive detector with a 75 mm diameter micro-channel plate coupled to a phosphor screen and a charge-coupled device (CCD) camera. A National Instrument PXI-mainframe system is used to control the whole apparatus and for data acquisition. The tunable detachment radiation (222–709 nm, linewidth <0.3 cm^{-1}) is from a Continuum Sunlite OPO system pumped by an injection-seeded Continuum Powerlite laser. A half-wave plate combined with a high-quality Glan-Laser polarizer is used to achieve a high degree of polarization parallel to the imaging detector plane. For the current work, photoelectron images were averaged with 50 000 to 200 000 laser shots and quadrant-symmetrized before inverse-Abel transformation to obtain the three-dimensional (3D) electron

a)E-mail: Lai-Sheng_Wang@brown.edu

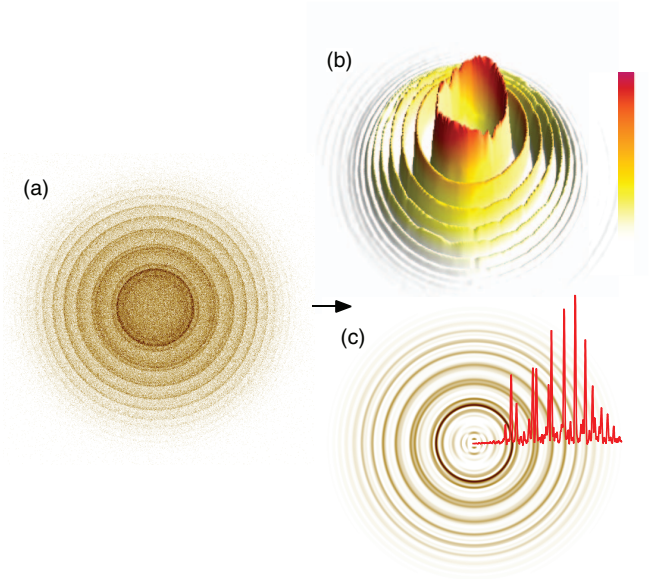

FIG. 1. Photoelectron images of Au_2^- taken at a photodetachment wavelength of 590.41 nm (2.1000 eV). (a) The raw image. (b) The 3D view of the raw image after inverse-Abel transformation. (c) The 2D view of the inverted image overlaid with the electron kinetic energy distribution obtained by integrating the electron counts circumferentially.

distributions from the recorded two-dimensional (2D) images. This reconstruction was done by both the BASEX[37] and pBASEX[38] programs, which yielded similar results. The imaging system was calibrated using the known spectrum of Au^-.

Figure 1 illustrates the reconstruction process of photoelectron images and the conversion from images to electron kinetic energies (KE $\propto r^2$, where r is the radius of the image). The image in Fig. 1 corresponds to detachment transitions from the ground electronic state of Au_2^- ($^2\Sigma_u^+$) to that of Au_2 ($^1\Sigma_g^+$) at a photon energy of 2.1000 eV (590.41 nm). Figure 1(a) shows the raw image, where the circles represent electrons with different kinetic energies or transitions to different vibrational levels of Au_2 in its ground electronic state. Figure 1(b) displays the 3D view of the image after the inverse-Abel transformation, while Fig. 1(c) is the 2D projection overlaid by the electron kinetic energy distributions obtained by integrating all electron counts circumferentially. The electron binding energy spectra presented in Figs. 2–4 are obtained by subtracting the electron kinetic energy spectra from the respective detachment photon energies. The photoelectron images shown in Fig. 1 are fairly isotropic, which are also the cases for all the images at lower photon energies (Fig. 4).

We showed previously that supersonic cooling was critical to obtain well-resolved photoelectron spectra by our magnetic-bottle apparatus for clusters produced from a laser vaporization source.[39] We found that the resident time of the cluster inside the nozzle was important to achieve better cooling, but we were not able to estimate the vibrational temperatures quantitatively. The vibrational resolution in the new imaging apparatus afforded us an opportunity to study the vibrational cooling for Au_2^-. Figure 2 displays the spectrum of Au_2^- at 442.80 nm (2.8000 eV) under the coldest conditions achievable for this cluster, in comparison with the Franck-Condon simulation using the Pescal program.[28,40] Because the resolution of SEVI depends on the electron kinetic energies, we fit the data in the electron velocity space and then converted both the experimental spectra and the simulation to the electron binding energy scale. The 442.80 nm

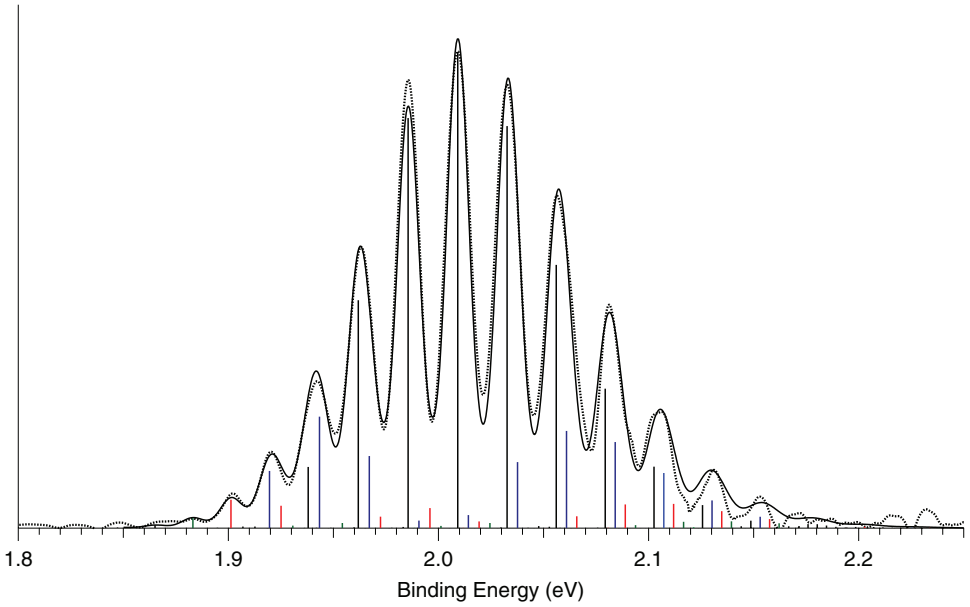

FIG. 2. Photoelectron spectrum of Au_2^- taken at 442.80 nm (2.8000 eV). The points represent the experimental data and the solid line is the Franck-Condon simulated spectrum. The vertical sticks represent the calculated Franck-Condon factors: black for $v \leftarrow 0'$, blue for $v \leftarrow 1'$, red for $v \leftarrow 2'$, and green for $v \leftarrow 3'$ transitions.

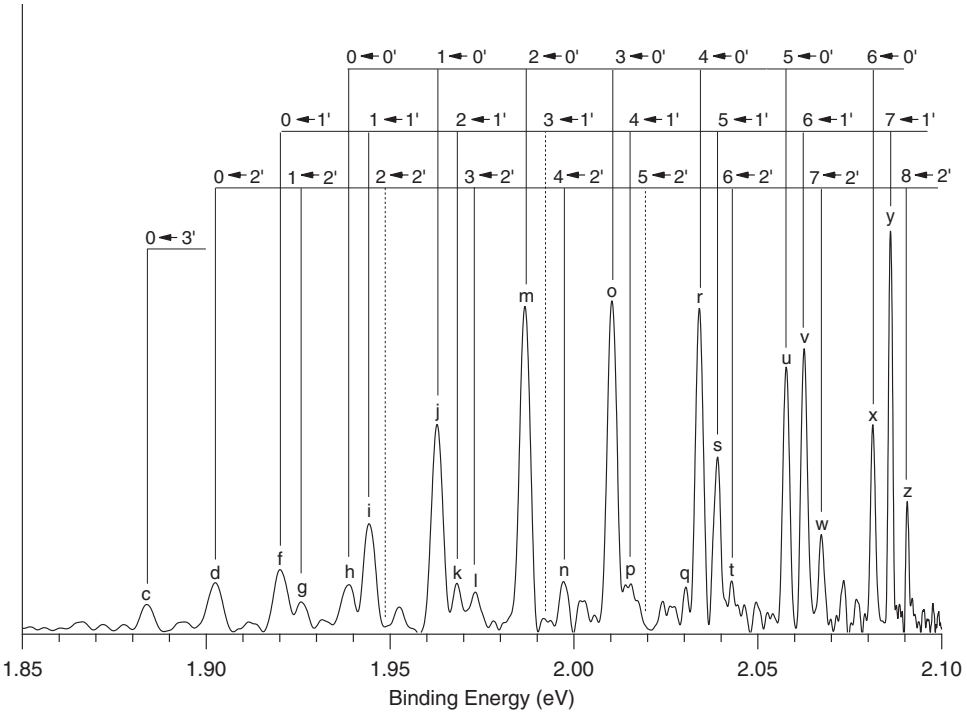

FIG. 3. Photoelectron spectrum of Au_2^- taken at 590.41 nm (2.1000 eV) together with the detailed vibrational assignments. The dashed lines indicate transitions with low or negligible Franck-Condon factors (see Fig. 2).

photon energy is high enough to allow the full Franck-Condon profile of the ground state detachment transition of Au_2^- to be observed with a resolution comparable to that reported in Ref. 28. The vibrational frequency and anharmonicity used for Au_2 are from Refs. 29 and 31, while those for the anion are from the current work (see below). The bond displacement and vibrational temperature were adjusted to give the best fit (Fig. 2). We obtained a vibrational temperature of 175 ± 25 K, similar to the 165 ± 30 K reported in Ref. 7. The equilibrium bond length (r_e) obtained for the anion was 1.587 Å, within the range of that reported in Ref. 28 (Table I).

Higher resolution spectra were measured at lower photon energies. Figure 3 shows the photoelectron spectrum at 590.40 nm, obtained from the photoelectron images of Fig. 1, together with the detailed assignments. Since the kinetic energy resolution of the imaging method increases for low energy electrons ($\Delta KE \propto r$ or $KE^{1/2}$), we measured the spectra of Au_2^- at lower photon energies with 0.05 eV increment down to 671.28 nm (1.8470 eV), as shown in Fig. 4, where some of the line widths are indicated. The best resolution we have achieved was 1.4 cm^{-1} for electrons with a kinetic energy of 6.1 cm^{-1} for atomic transitions. The accuracy for the peak position measurement also increases with decreasing electron kinetic energies. We can achieve an accuracy of ± 0.6 meV for electrons with kinetic energies less than 50 meV, including both the uncertainty in the spectral calibration and the uncertainty of the laser wavelengths. The binding energies of all the observed transitions (Table S1)[41] were measured from the spectra at the lowest photon energies.

The electron affinity (EA) of Au_2 was determined as 1.9393 ± 0.0006 eV from the $0 \leftarrow 0'$ transition (peak *h* in Figs. 3 and 4). This value was measured from the low photon energy spectra at 635.82 nm (Fig. 4(c)) and 619.92 nm (Fig. 4(d)). The current result represents the most accurate EA value for Au_2, as compared with the two previous measurements in Table I. The peaks observed in the spectra at 652.55 nm (Fig. 4(b)) and 671.28 nm (Fig. 4(a)) are entirely due to vibrational hot bands of Au_2^-. The lowest binding energy peak observed (a′ in Fig. 4(a)) corresponds to $0 \leftarrow 6'$ (Table S1).[41] We estimated a population of ~0.1% for the $v' = 6$ vibrational level of Au_2^- at $T_{vib} \sim 200$ K. That this transition was observed at all indicates the sensitivity of the imaging technique. The observation of this weakly populated vibrational hot band was also benefitted from the fact that there was no background noise at this low photon energy. The spectra shown in Figs. 3 and 4 also reveal a threshold enhancement phenomenon for the peaks on the very high binding energy side at each photon energy. For example, the peak labeled as *y* in Fig. 3, corresponding to the $7 \leftarrow 1'$ transition, is much more intense than the calculated Franck-Condon factor (Fig. 2). A long-lived excited state was observed previously for Au_2^-, with an excitation energy slightly above the detachment threshold.[42] Autodetachment can happen via this excited state, giving rise to the anomalous intensities near threshold. A similar argument has been invoked previously to explain anomalous vibrational intensities in photoelectron imaging of C_4H^-.[43] In addition, the Wigner threshold law favors near threshold detachments with s-outgoing waves,[9] which has been observed in SEVI previously.[44]

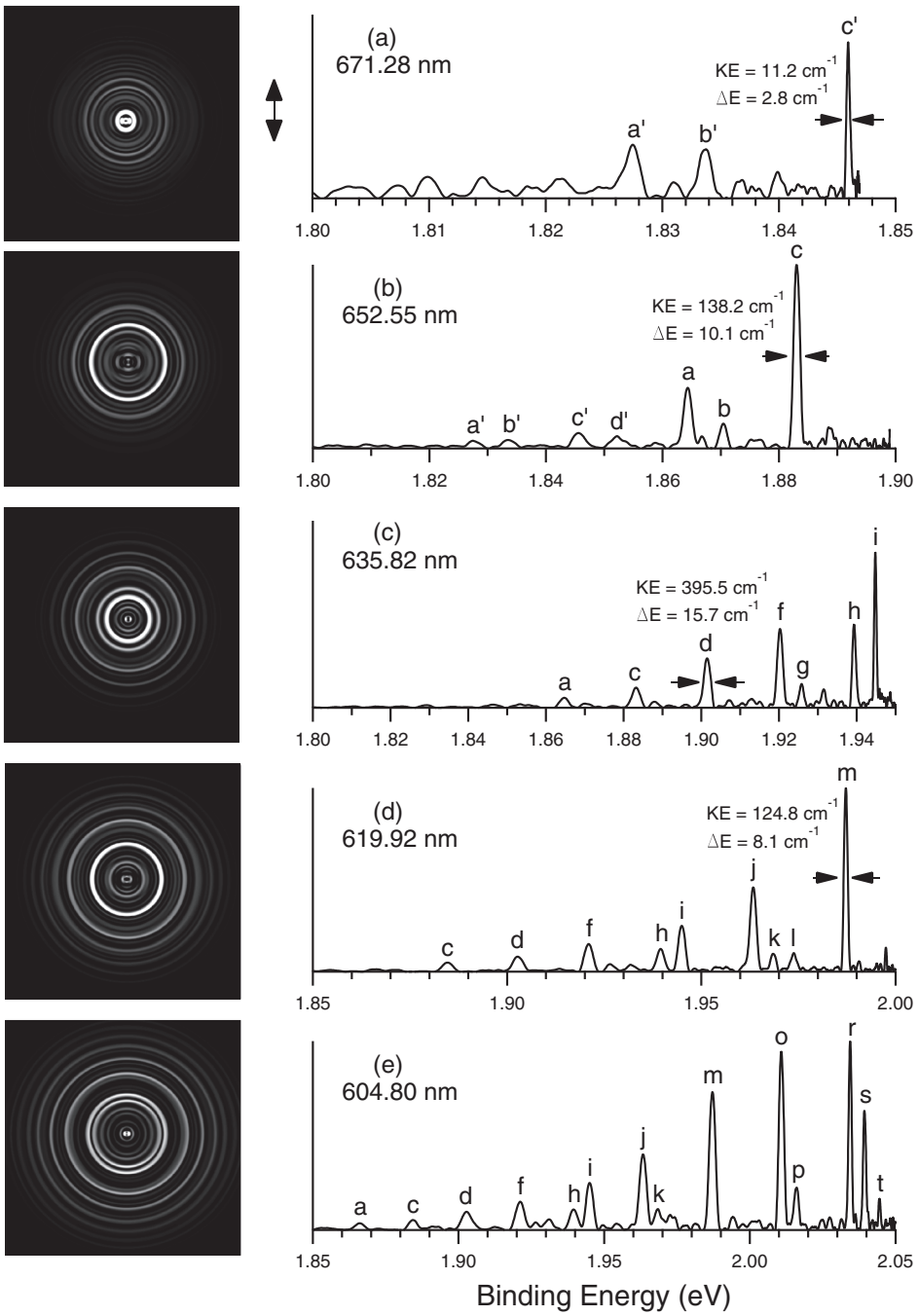

FIG. 4. Photoelectron images and spectra of Au_2^- at different detachment photon energies: (a) 671.28 (1.8470 eV), (b) 652.55 (1.9000 eV), (c) 635.82 nm (1.9500 eV), (d) 619.92 (2.0000 eV), and (e) 604.80 nm (2.050 eV). The left panel shows the photoelectron images after the inverse-Abel transformation. The double arrow in (a) indicates the polarization of the laser. The kinetic energy and the corresponding peak width (FWHM) for some of the peaks are also shown.

We fitted the observed vibrational spacings for both the anionic and neutral ground state of Au_2 to an anharmonic oscillator described by the Morse potential and obtained a relatively accurate harmonic vibrational frequency and anharmonicity for Au_2^-, as given in Table I along with literature values. Furthermore, using the accurate EA value measured in this work together with a redefinition of the dissociation energy for Au_2 by Morse and coworkers,[31] we obtained a more accurate dissociation energy for the ground state of Au_2^- as 1.937 ± 0.005 eV (Table I).

In conclusion, we report high resolution photoelectron spectra of Au_2^- using a newly built photoelectron imaging instrument. Accurate spectroscopic constants are obtained for the ground electronic state of Au_2^-, as well as a more accurate electron affinity for Au_2. Even with a relatively cold cluster beam, photodetachment transitions from $v' = 6$ from Au_2^- were observed due to the high sensitivity

TABLE I. The obtained spectroscopic constants for Au_2 and Au_2^-, in comparison with those from the literature.

	Au_2 ($X\,^1\Sigma_g^+$)		Au_2^- ($X\,^2\Sigma_u^+$)	
	Current work	Literature	Current work	Literature
EA (eV)	1.9393 ± 0.0006	1.938 ± 0.007[a] 1.940 eV ± 0.5 meV[b]		
ω_e (cm^{-1})	194 ± 9	190.9[c]	153 ± 8	149 ± 10[a]
$\omega_e x_e$ (cm^{-1})	[0.41][d]	0.42[c]	[0.44][d]	[0.7][a]
D_0 (eV)		2.290 ± 0.008[e] 2.301–2.311[c]	1.937 ± 0.005[f]	1.92 ± 0.15[a]
r_e (Å)		2.4715[g]	1.587	1.582 ± 0.007[a]

[a]From Ref. 28.
[b]From Ref. 7.
[c]From Ref. 31.
[d]The values in brackets are estimates from this work.
[e]From Ref. 30.
[f]Calculated by the relationship: $D_0\ (Au_2^-) = D_0\ (Au_2) + EA\ (Au_2) - EA\ (Au)$. The $D_0\ (Au_2)$ value is from Ref. 31, the EA (Au_2) value is from the current work, and the EA (Au) is from Ref. 45.
[g]From Ref. 29.

of the imaging method. The high resolution capability of the imaging method should allow accurate vibrational and electronic information to be obtained for a broad range of size-selected atomic clusters.

I.L. thanks the Basque Government for a postdoctoral fellowship. We are grateful to Dr. G. Garcia for sharing the pBasex program. This work was supported by the National Science Foundation (NSF) (CHE-1049717).

[1]K. Muller-Dethlefs, M. Sander, and E. W. Schlag, Chem. Phys. Lett. **112**, 291 (1984).
[2]M. Sander, L. A. Chewter, K. Muller-Dethlefs, and E. W. Schlag, Phys. Rev. A **36**, 4543 (1987).
[3]D. S. Yang and P. A. Hackett, J. Electron Spectrosc. Relat. Phenom. **106**, 153 (2000).
[4]Y. X. Lei, L. Wu, B. R. Sohnlein, and D. S. Yang, J. Chem. Phys. **136**, 204311 (2012).
[5]T. N. Kitsopoulos, I. M. Waller, J. G. Loeser, and D. M. Neumark, Chem. Phys. Lett. **159**, 300 (1989).
[6]C. C. Arnold and D. M. Neumark, J. Chem. Phys. **99**, 3353 (1993).
[7]G. F. Gantefor, D. M. Cox, and A. Kaldor, J. Chem. Phys. **93**, 8395 (1990).
[8]G. Drechsler, C. Bassmann, U. Boesl, and E. W. Schlag, J. Mol. Struct. **348**, 337 (1995).
[9]E. P. Wigner, Phys. Rev. **73**, 1003 (1948).
[10]D. W. Chandler and P. L. Houston, J. Chem. Phys. **87**, 1445 (1987).
[11]H. Helm, N. Bjerre, D. J. Dyer, D. L. Huestis, and M. Saeed, Phys. Rev. Lett. **70**, 3221 (1993).
[12]C. Pinare, B. Baguenard, C. Bordas, and M. Broyer, Phys. Rev. Lett. **81**, 2225 (1998).
[13]A. T. J. B. Eppink and D. H. Parker, Rev. Sci. Instrum. **68**, 3477 (1997).
[14]H. J. Deyerl, L. S. Alconcel, and R. E. Continetti, J. Phys. Chem. A **105**, 552 (2001).
[15]E. Surber and A. Sanov, J. Chem. Phys. **116**, 5921 (2002).
[16]A. V. Davis, R. Wester, A. E. Bragg, and D. M. Neumark, J. Chem. Phys. **118**, 999 (2003).
[17]G. J. Rathbone, T. Sanford, D. Andrews, and W. C. Lineberger, Chem. Phys. Lett. **401**, 570 (2005).
[18]M. A. Sobhy and A. W. Castleman, Jr., J. Chem. Phys. **126**, 154314 (2007).
[19]L. R. Mccunn, G. H. Gardenier, T. L. Guasco, B. M. Elliott, J. C. Bopp, R. A. Relph, and M. A. Johnson, J. Chem. Phys. **128**, 234311 (2008).
[20]X. Wu, Z. B. Qin, H. Xie, R. Cong, X. H. Wu, Z. C. Tang, and H. J. Fan, J. Chem. Phys. **133**, 044303 (2010).
[21]A. Osterwalder, M. J. Nee, J. Zhou, and D. M. Neumark, J. Chem. Phys. **121**, 6317 (2004).
[22]S. J. Cavanagh, S. T. Gibson, M. N. Gale, C. J. Dedman, E. H. Roberts, and B. R. Lewis, Phys. Rev. A **76**, 052708 (2007).
[23]D. M. Neumark, J. Phys. Chem. A **112**, 13287 (2008).
[24]P. Hockett, M. Staniforth, and K. L. Reid, Phys. Rev. Lett. **102**, 253002 (2009).
[25]X. P. Xing, X. B. Wang, and L. S. Wang, Phys. Rev. Lett. **101**, 083003 (2008).
[26]X. P. Xing, X. B. Wang, and L. S. Wang, J. Chem. Phys. **130**, 074301 (2009).
[27]M. D. Morse, Chem. Rev. **86**, 1049 (1986).
[28]J. Ho, K. Ervin, and W. C. Lineberger, J. Chem. Phys. **93**, 6987 (1990).
[29]B. Simard and P. A. Hackett, J. Mol. Spectrosc. **142**, 310 (1990).
[30]G. A. Bishea and M. D. Morse, J. Chem. Phys. **95**, 5646–5659 (1991).
[31]A. M. James, P. Kowalczyk, B. Simard, J. C. Pinegard, and M. D. Morse, J. Mol. Spectrosc. **168**, 248 (1994).
[32]W. S. Hopkins, S. M. Hamilton, P. D. McNaughter, and S. R. Mackenzie, Chem. Phys. Lett. **483**, 10 (2009).
[33]K. R. Geethalakshmi, F. Ruiperez, S. Knecht, J. M. Ugalde, M. D. Morse, and I. Infante, Phys. Chem. Chem. Phys. **14**, 8732 (2012).
[34]L. S. Wang, H. S. Cheng, and J. W. Fan, J. Chem. Phys. **102**, 9480 (1995).
[35]W. Huang and L. S. Wang, Phys. Rev. Lett. **102**, 153401 (2009).
[36]D. Townsend, M. P. Minitti, and A. G. Suits, Rev. Sci. Instrum. **74**, 2530 (2003).
[37]V. Dribinski, A. Ossadtchi, V. A. Mandelshtam, and H. Reisler, Rev. Sci. Instrum. **73**, 2634 (2002).
[38]G. A. Garcia, L. Nahon, and I. Powis, Rev. Sci. Instrum. **75**, 4989 (2004).
[39]J. Akola, M. Manninen, H. Hakkinen, U. Landman, X. Li, and L. S. Wang, Phys. Rev. B **60**, R11297 (1999).
[40]K. M. Ervin, PESCAL, Fortran program, 2010.
[41]See supplementary material at http://dx.doi.org/10.1063/1.4803477 for the listing of the binding energies of all the observed transitions and their assignments.
[42]G. F. Gantefor, D. M. Cox, and A. Kaldor, J. Chem. Phys. **94**, 854 (1991).
[43]J. Zhou, E. Garand, and D. M. Newmark, J. Chem. Phys. **127**, 154320 (2007).
[44]E. Garand, K. Klein, J. F. Stanton, J. Zhou, T. I. Yacovitch, and D. M. Newmark, J. Phys. Chem. A **114**, 1374 (2010).
[45]J. C. Rienstra-Kiracofe, G. S. Tschumper, H. F. Schaefer III, S. Nandi, and G. B. Ellison, Chem. Rev. **102**, 231 (2002).